AIP | Journal of Applied Physics

Magnetoplasmonic nanostructures based on nickel inverse opal slabs

A. A. Grunin, N. A. Sapoletova, K. S. Napolskii, A. A. Eliseev, and A. A. Fedyanin

Citation: J. Appl. Phys. **111**, 07A948 (2012); doi: 10.1063/1.3680175
View online: http://dx.doi.org/10.1063/1.3680175
View Table of Contents: http://jap.aip.org/resource/1/JAPIAU/v111/i7
Published by the American Institute of Physics.

Magnetoplasmonic nanostructures based on nickel inverse opal slabs

A. A. Grunin,[1] N. A. Sapoletova,[2] K. S. Napolskii,[2] A. A. Eliseev,[2] and A. A. Fedyanin[1,a)]
[1]*Faculty of Physics, Lomonosov Moscow State University, Moscow 119991, Russia*
[2]*Faculty of Material Science, Lomonosov Moscow State University, Moscow 119991, Russia*

(Presented 31 October 2011; received 23 September 2011; accepted 23 December 2011; published online 13 March 2012)

Nanostructured nickel surfaces representing periodically arranged spherical voids in a nickel film are obtained by electrochemical deposition through a self-assembled opaline template. Excitation of surface plasmon-polaritons (SPPs) on the surface of the sample is experimentally observed as the Wood's anomaly in the reflectance spectra. Transversal magneto-optical Kerr effect (TMOKE) spectra are measured at the different angles of incidence and azimuthal angles. The two- to-threefold enhancement of TMOKE caused by the excitation of mixed plasmons in two selected azimuthal configurations is observed. © *2012 American Institute of Physics*. [doi:10.1063/1.3680175]

I. INTRODUCTION

Active plasmonics is a modern and rapidly developing area of research because it is promising for creation devices for integral photonics and plasmonics. One of the ways to control propagation of surface plasmons is application of magnetic field in transversal geometry (Voigt geometry) that allows changing their wavevector k. In this case, surface plasmons are called magnetoplasmons,[1,2] but relative changes in the wavevector do not exceed 10^{-3} in the optical spectra range for ferromagnetic metals. The modulation of wavevector of surface plasmons leads to enhancement of transversal magneto-optical Kerr effect (TMOKE), which has been recently observed in nickel nanogratings,[3] in ferrite-garnet-noble metal grating[4] or in Au/Co/Au multilayer structures.[5] These magnetoplasmonic structures support both magneto-optical and plasmonic properties and allow using TMOKE as a probing tool for surface plasmon-polaritons (SPPs).[2] Recently, interesting plasmonic effects, such as excitation of localized (Mie) and delocalized (Bragg) surface plasmons and plasmonic bandgap, were observed in nanostructures fabricated by electrodeposition of noble metals using polystyrene colloidal crystal as a template.[6] In this paper, the results of fabrication of nickel inverse opal slabs and systematic studies of TMOKE in the spectral range of localized and delocalized plasmons excitation are presented.

II. EXPERIMENT

Nickel inverse opal slabs were prepared by electrodeposition of nickel into the voids of artificial opals.[7,8] Artificial opals were prepared by an electric-field-assisted vertical deposition of monodisperse polystyrene microspheres (mean sphere diameter is $D = 600$ nm; relative standard deviation (RSD) $< 10\%$) onto silicon (100) wafers PVD coated with a 200-nm-thick gold layer.[9] Electrodeposition of nickel was carried out in the three-electrode cell from aerated 0.6 M $NiSO_4$ + 0.1 M $NiCl_2$ + 0.3 M H_3BO_3 + 3.5 M C_2H_5OH electrolyte at room temperature. The colloidal crystal film on the conducting support was vertically aligned at a distance of 3 cm from the Pt counterelectrode and acts as a working electrode during electrodeposition. The reference electrode was a saturated aqueous Ag/AgCl electrode connected to the cell via a Luggin capillary. Electrodeposition was carried out in a potentiostatic mode at the deposition potential of −0.9 V. The samples with a different normalized thickness $t = 0.1$, 0.6, and 0.9 were prepared. Normalized thickness of samples t was defined as $t = h/D$, where h is thickness of the sample [see Fig. 1(c)]. The areas of the samples with $t = 0.1$, 0.6, and 0.9 were 0.3, 0.25, and 0.4 cm^2, correspondingly. In order to obtain free-standing metallic structures on the supports, the polystyrene microspheres were later dissolved in toluene for 3 h. The period of the inverse opal slabs, $d = 520$ nm, and diameter of microspheres, $D = 600$ nm were determined by laser diffraction technique.

The TMOKE was measured by using a saturated external ac magnetic field oscillating at a frequency of 75 Hz with the amplitude $H \simeq 600$ Oe, a halogen lamp with a monochromator as a light source, and a lock-in detector with a silicon detector. Magnetic field was oriented in the sample plane and perpendicular to the plane of incidence. Polarization of the incident light was in the incident plane (p-polarization). Azimuthal angle ψ, which is defined as the angle between the plane of incidence and one of the reciprocal vectors and the angle of incidence θ, was step-motor controlled.

III. RESULTS AND DISCUSSION

A typical SEM image of the nickel inverse opal slab is shown in Fig. 1(a) and the schematic of its periodic lattice is shown in Fig. 1(b). The inverse opal surface has sixfold symmetry and plasmonic properties are determined by two reciprocal vectors $\mathbf{G}_1$ and $\mathbf{G}_2$ with absolute values of $G = 2\pi/d$. The use of subwavelength metal grating allows the fulfillment of phase-matching conditions for SPPs excitation at metallic surface.[3] The surface of inverse opal represents two-dimensional subwavelength metal grating. Thus, the phase-matching condition between the incident electromagnetic wave and the propagating SPP is written as follows: $-\mathbf{k}_{spp} = \mathbf{k}_{||} + n\mathbf{G}_1 + m\mathbf{G}_2$, where $\mathbf{k}_{spp}$ is the SPP

a)Electronic mail: fedyanin@nanolab.phys.msu.ru.

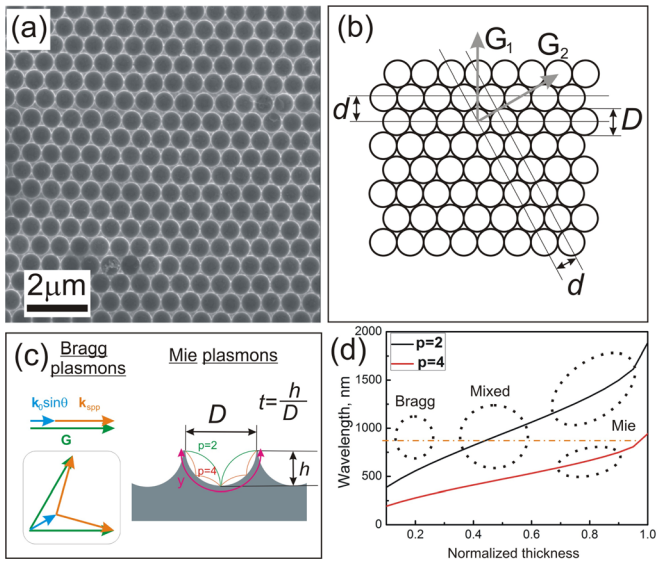

FIG. 1. (Color online) (a) SEM image of a surface of nickel inverse opal slab. (b) Hexagonal grating representing surface periodicity of the structure and its reciprocal vectors $\mathbf{G}_1$, $\mathbf{G}_2$; D is a diameter of microspheres in opal matrix, $d = \sqrt{3}/2D$ is period of the grating. (c) Schematic of excitation of delocalized (left) and localized plasmons (right) and the definition of normalized thickness t. (d) The dependence of localized and delocalized plasmon wavelengths for $\theta = 45^\circ$ and $\psi = 0^\circ$ on normalized thickness t calculated for $D = 600$ nm, $d = 520$ nm. Three areas corresponded to excitation of Bragg, mixed, and Mie plasmons are shown.

wavevector, $\mathbf{k}_\parallel$ is projection of the incident radiation wavevector onto metal surface, and n and m are integers. Such plasmons propagate along the metal surface and are called delocalized or Bragg plasmons.[6] The Bragg plasmons excitation depends on the angle of incidence θ and azimuthal angle ψ (the angle between incidence plane and reciprocal vector $\mathbf{G}_1$) and is observed as Wood's anomaly, which is the minimum in reflection spectra of p-polarized light due to the redistribution of incident energy to surface plasmons. There are two specific cases of Bragg plasmon excitation on sixfold symmetry metallic surface, $\psi = 0^\circ$ and $\psi = 30^\circ$, which are depicted in the vectorial form in Fig. 1(c).

Another type of surface plasmons excited in metallic nanovoids is localized or Mie plasmons.[6,10,11] One approach to modeling the plasmon modes of a truncated void is to consider localized plasmon as plasmon-polariton standing wave within the dish,[6] which is schematically shown in Fig. 1(c). Excitation condition for Mie plasmons can be written in the one-dimensional model as follows: $k_{\mathrm{loc}} = \frac{\pi p}{D\arccos(1-2t)}$, where p is an integer corresponding to the number of half-wavelengths fitted into the curved rim-to-rim distance y. Dependences of excitation wavelength for Mie plasmons for $p = 2,4$ and Bragg plasmons for $\theta = 45^\circ$, $\psi = 0^\circ$ on normalized thickness t is shown in Fig. 1(d). A crosspoint of dispersion curves of Bragg and Mie plasmons leads to appearance of plasmonic bandgap, strong plasmon modes interaction and mixed plasmon excitation.[10] Three areas corresponding to excitation of pure Bragg plasmons, mixed plasmons, and pure Mie plasmons in the desired spectral range can be identified in Fig. 1(d), all of them being realized using nickel inverse opal slabs with normalized thicknesses of $t = 0.1$, 0.6, and 0.9.

Reflection and TMOKE value δ spectra of nickel inverse opal slabs with $t = 0.1$, 0.6, and 0.9 in comparison with TMOKE spectra of plain nickel film are shown in Fig. 2. TMOKE value δ is defined as $\delta = (I(H) - I(-H))/I_0$, where $I(H)$ and I_0 are reflected light intensities with and without external magnetic field, respectively. Strong peculiarities in TMOKE spectra are observed only for the sample with $t = 0.6$. The TMOKE value of plain nickel for wavelengths larger than 800 nm is treated as negative, thus the dip in the TMOKE spectra of inverse opal slabs indicates an increase of the magneto-optical effect correlated with the dip in reflection. Experimental angular dependence of the plasmon excitation wavelength for this sample is slightly shifted relative to the dependence calculated in the model of Bragg plasmons shown in Eq. 1. The dip in reflection spectrum of the sample with $t = 0.1$ is not observed in the wavelengths range corresponding to Bragg plasmon excitations, and the effect of strong TMOKE enhancement was not detected contrary to the case of nickel nanogratings.[3] However, even for gold inverse opal slabs[6] with $t \simeq 0.1$, pure Bragg plasmons are also not efficiently excited under non-normal angles of incidence. Peculiarities observed in reflection spectra of the sample with $t = 0.9$, such as peak at $\lambda = 750$ nm and dip at $\lambda = 900$ nm with spectral positions independent on the angle of incidence, are due to excitation of Mie plasmons. Their excitation leads to weak changes in TMOKE due to the weak

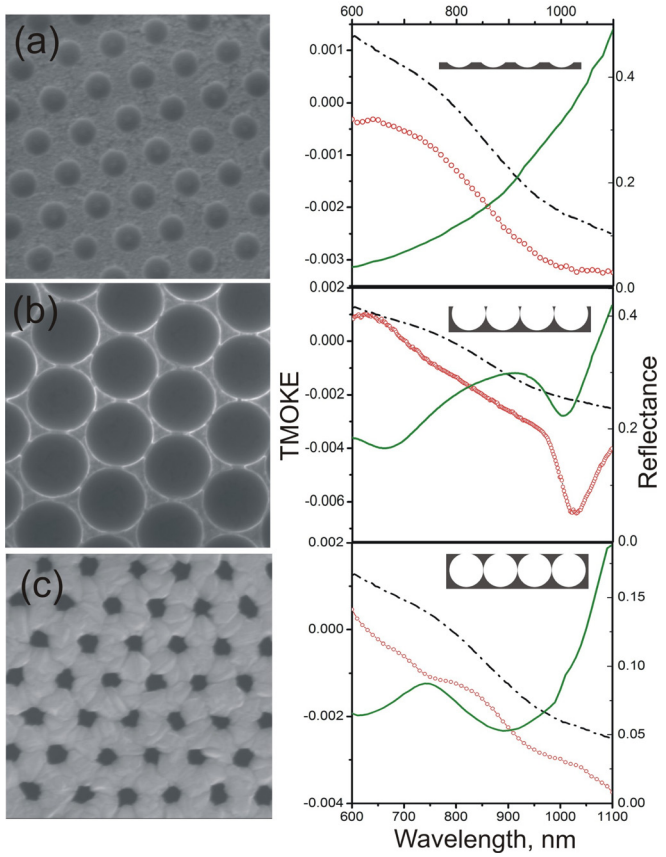

FIG. 2. (Color online) TMOKE value (circles) and reflection (solid curve) spectra at $\theta = 60^\circ$ and $\psi = 0^\circ$ measured in inverse nickel opal slabs with different t values: (a) $t = 0.1$, (b) $t = 0.6$, (c) $t = 0.9$. Reference TMOKE spectra of plain nickel film measured under the same conditions are shown by dashed–dotted curve.

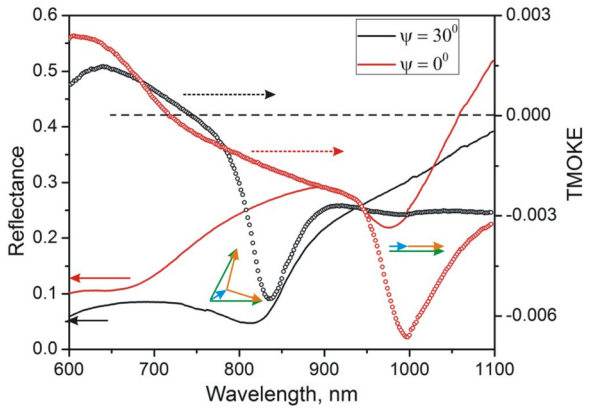

FIG. 3. (Color online) Reflection and TMOKE spectra of nickel inverse opal with $t = 0.6$ slabs measured for $\theta = 50°$ and $\psi = 0°$ and $\psi = 30°$. Grouped arrows depict conditions for excitation of delocalized plasmons for $\psi = 0°$ and $\psi = 30°$.

dependence of dispersion law of localized plasmons on magnetic field.

Figure 3 shows spectral dependences of the reflectance and TMOKE value measured in the nickel inverse opal slab with $t = 0.6$ at $\theta = 50°$ for two azimuthal orientations, $\psi = 0°$ and $\psi = 30°$. The dip in reflection spectrum is shifted in the short-wavelength range under increasing of the azimuthal angle. The excitation of SPPs in these two azimuthal configurations can be described as excitation of Bragg plasmons with collinear and symmetrical non-collinear phase-matching conditions depicted by arrows in Fig. 3. TMOKE spectra shows two to three times enhancement in comparison with the plain nickel film in the spectral vicinity of the dips in reflection spectra corresponding to the SPP excitation. The peak of TMOKE is spectrally located at the right edge of the reflection dip and has a symmetrical line shape contrary to the case of nickel nanogratings.[3] Both magneto-optical spectra also show the trend of the TMOKE value decreasing with the wavelength increase associated with the spectral dependence of the nickel gyration constant.

TMOKE enhancement can be phenomenologically interpreted as a result of the SPP dispersion curve shift upon the magnetization reversal in magnetic media. The dip in reflection spectra is also shifted because of the change of the SPP phase-matching condition. As the TMOKE effect is proportional to the difference between reflection coefficients for opposite magnetization directions normalized to the mean reflection coefficient, the resonant part of the TMOKE spectrum is proportional to the derivative of reflection spectra.[2,3] The derivatives at the left and right edges of reflection dip have different signs that lead to asymmetrical Fano shape of the TMOKE spectrum in nickel nanograting.[3] The derivative of reflection spectra at the right edge of the dip is larger than that at the left edge, leading to the symmetrical shape of the TMOKE spectrum at plasmonic resonance in a nickel inverse opal slab. Therefore, reflection and TMOKE spectra for the sample with $t = 0.6$ for azimuthal orientations $\psi = 0°$ and $\psi = 30°$ are well described by the Bragg plasmons model.

The dependences of reflection and TMOKE spectra on azimuthal angle measured in the nickel inverse opal slab with $t = 0.6$ at $\theta = 45°$ are shown in Fig. 4. The position of

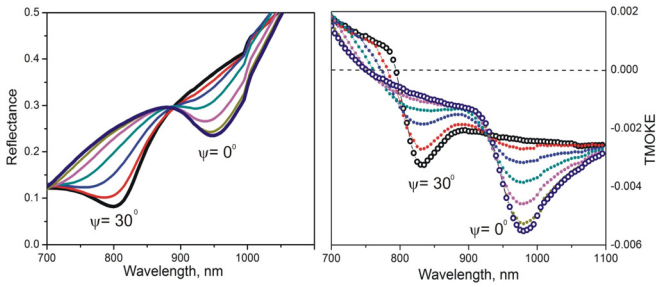

FIG. 4. (Color online) Reflection (left) and TMOKE (right) spectra of nickel inverse opal slabs measured at $\theta = 45°$ for azimuthal angles ψ with 5° steps in the interval at least from 0° to 30°.

the reflection dip does not tune continuously under the changing of azimuthal angles as it follows from the Bragg plasmons model described by Eq. 1. Surface plasmons are excited efficiently only in two selected azimuthal orientations, $\psi = 0°$ and $\psi = 30°$. This difference from the Bragg plasmons proves a mixed origin of these plasmonic excitations. The efficient enhancement of TMOKE is also observed only in these two selected azimuthal orientations.

In conclusion, the two time enhancement of TMOKE is observed in a nickel inverse opal slab with normalized thickness $t = 0.6$ in the spectral range of surface plasmon excitation for two selected azimuthal configurations. The maximum of the TMOKE value is located at the right edge of the reflection dip. The excitation of Mie plasmons does not lead to significant changes in TMOKE.

ACKNOWLEDGMENTS

The work was has been supported in part by grants of Samsung Advanced Institute of Technology (SAIT) project (Grant No 10-001), Russian Foundation of Basic Research Grant No. 11-02-92009 and Russian Ministry of Education and Science Grant No. P946.

[1]M. S. Kushwaha and P. Halevi, Phys. Rev. B **36**, 5960 (1987).
[2]G. Armelles, A. Cebollada, A. Garcia-Martin, J. M. Garcia-Martin, M. U. Gonzalez, J. B. Gonzalez-Diaz, E. Ferreiro-Vila, and J. F. Torrado, J. Opt. A, Pure Appl. Opt. **11**, 114023 (2009).
[3]A. A. Grunin, A. G. Zhdanov, A. A. Ezhov, E. A. Ganshina, and A. A. Fedyanin, Appl. Phys. Lett. **97**, 261908 (2010).
[4]V. I. Belotelov, I. A. Akimov, M. Pohl, V. A. Kotov, S. Kasture, A. S. Vengurlekar, A. V. Gopal, D. R. Yakovlev, A. K. Zvezdin, and M. Bayer, Nature Nanotech. **6**, 370 (2011).
[5]C. Clavero, K. Yang, J. R. Skuza, and R. A. Lukaszew, Opt. Exp. **18**, 7743 (2010).
[6]T. A. Kelf, Y. Sugawara, R. M. Cole, J. J. Baumberg, M. E. Abdelsalam, S. Cintra, S. Mahajan, A. E. Russell, and P. N. Bartlett, Phys. Rev. B **74**, 245415 (2006).
[7]K. S. Napolskii, A. Sinitskii, S. V. Grigoriev, N. A. Grigorieva, H. Eckerlebe, A. A. Eliseev, A. V. Lukashin, and Y. D. Tretyakov, Physica B **23**, 397 (2007).
[8]N. Sapoletova, T. Makarevich, K. Napolskii, E. Mishina, A. Eliseev, A. van Etteger, T. Rasing, G. Tsirlina, Phys. Chem. Chem. Phys. **12**, 15414 (2010).
[9]K. S. Napolskii, N. A. Sapoletova, D. F. Gorozhankin, A. A. Eliseev, D. Y. Chernyshov, D. V. Byelov, N. A. Grigoryeva, A. A. Mistonov, W. G. Bouwman, K. O. Kvashnina, A. V. Lukashin, A. A. Snigirev, A. V. Vassilieva, S. V. Grigoriev, and A. V. Petukhov, Langmuir **26**, 2346 (2010).
[10]T. A. Kelf, Y. Sugawara, J. J. Baumberg, M. E. Abdelsalam, and P. N. Bartlett, Phys. Rev. Lett. **95**, 116802 (2005).
[11]T. V. Teperik, V. V. Popov, F. J. Garcia de Abajo, T. Kelf, Y. Sugawara, J. J. Baumberg, M. E. Abdelsalam, and P. N. Bartlett, Opt. Express **14**, 11964 (2006).